

## 'Wrong bonds' in sputtered amorphous $\text{Ge}_2\text{Sb}_2\text{Te}_5$

This article has been downloaded from IOPscience. Please scroll down to see the full text article.

2007 J. Phys.: Condens. Matter 19 335212

(<http://iopscience.iop.org/0953-8984/19/33/335212>)

View [the table of contents for this issue](#), or go to the [journal homepage](#) for more

Download details:

IP Address: 129.252.86.83

The article was downloaded on 28/05/2010 at 19:59

Please note that [terms and conditions apply](#).

# ‘Wrong bonds’ in sputtered amorphous $\text{Ge}_2\text{Sb}_2\text{Te}_5$

P Jávári<sup>1,6</sup>, I Kaban<sup>2</sup>, J Steiner<sup>3</sup>, B Beuneu<sup>4</sup>, A Schöps<sup>5</sup> and A Webb<sup>5</sup>

<sup>1</sup> Research Institute for Solid State Physics and Optics, Hungarian Academy of Sciences, Budapest POB 49, H-1525 Hungary

<sup>2</sup> Institute of Physics, Chemnitz University of Technology, D-09107 Chemnitz, Germany

<sup>3</sup> Institute of Physics (IA), RWTH Aachen, 52056 Aachen, Germany

<sup>4</sup> Laboratoire Léon Brillouin CEA/Saclay, 91191 Gif-Sur-Yvette Cedex, France

<sup>5</sup> HASYLAB am Deutschen Elektronen Synchrotron, DESY, Notkestrasse 85, D-22603 Hamburg, Germany

E-mail: [jovari@sunserv.kfki.hu](mailto:jovari@sunserv.kfki.hu)

Received 9 February 2007

Published 4 July 2007

Online at [stacks.iop.org/JPhysCM/19/335212](http://stacks.iop.org/JPhysCM/19/335212)

## Abstract

The structure of sputtered amorphous  $\text{Ge}_2\text{Sb}_2\text{Te}_5$  was investigated by high energy x-ray diffraction, neutron diffraction and Ge-, Sb- and Te K-edge EXAFS measurements. The five datasets were modelled simultaneously in the framework of the reverse Monte Carlo simulation technique. It was found that apart from Te–Sb and Te–Ge bonds existing in the crystalline phases, Ge–Ge and Sb–Ge bonding is also significant in sputtered amorphous  $\text{Ge}_2\text{Sb}_2\text{Te}_5$ . According to our results, all components obey the ‘8-N’ rule.

## 1. Introduction

Since the first report on laser induced phase change in telluride films, which is based on the rapid and reversible change between the crystalline and glassy states [1], the physical properties of telluride films (reflectivity, resistance, density, phase transition kinetics) have been intensely investigated [2–5]. Despite the technological importance, relatively little is known about the atomic level structure in the amorphous and liquid states of phase change alloys. This is due to the fact that the number of parameters describing the short range order of a disordered system (bond lengths and coordination numbers) rises steeply with the number of components.

The  $\text{Ge}_2\text{Sb}_2\text{Te}_5$  alloy is used in digital versatile disc random access memory (DVD-RAM) as the recording medium due to its featuring characteristics—large reflectivity changes, short amorphization and crystallization time. The structure of amorphous  $\text{Ge}_2\text{Sb}_2\text{Te}_5$  is often described in terms of some characteristic units or building blocks. Such pictures can be very useful for simpler glasses where available experimental evidence allows for a detailed structural description but can be misleading if they are applied *instead of* setting up consistent models.

Kolobov *et al* suggested [6] that the amorphization of  $\text{Ge}_2\text{Sb}_2\text{Te}_5$  is accompanied by the jump of Ge atoms from octahedral to tetrahedral positions. Thus basic motifs of the amorphous

<sup>6</sup> Author to whom any correspondence should be addressed.

structure are the  $\text{GeTe}_{4/2}$  tetrahedra. Though this model is appealing in its simplicity some objections should be made here:

- (i) The model proposed in [6] is based on a wide range of experimental techniques. The argumentation is, however, rather qualitative. Methods such as Raman scattering or DSC do give useful information on structure but they cannot replace more direct and quantitative structural techniques. It is especially surprising that while interatomic distances determined by modelling EXAFS curves are used as ultimate arguments for the validity of the model, coordination numbers obtainable by the same type of analysis are *not* reported. Thus it is not shown that  $\text{GeTe}_{4/2}$  units can be found in the disordered state.
- (ii) On the evidence of Sb K-edge XANES data it is stated that ‘the local arrangement of atoms around Sb remains essentially unchanged’. According to reference [7], the first peak of the Sb–Te pair distribution function does not split up in cubic  $\text{Ge}_2\text{Sb}_2\text{Te}_5$  and the displacement of Sb atoms from their crystallographic positions is also significantly smaller than that of Ge atoms. These observations suggest that the Sb–Te coordination number is close to 6, the value characterizing the rocksalt structure. According to EXAFS studies on amorphous  $\text{Sb}_3\text{Te}$  [8] and  $\text{Pd}_1\text{Ge}_{17}\text{Sb}_{26}\text{Te}_{56}$  [9] Sb is threefold coordinated within experimental uncertainties. Thus the above statement contradicts both chemical intuition and previous results on amorphous chalcogenides.

More recently two EXAFS studies have been devoted to the structure of amorphous  $\text{Ge}_2\text{Sb}_2\text{Te}_5$  [10, 11]. They are based on the analyses of the same measurements and were published by the same group of authors. Somewhat disturbingly there are still significant differences in the findings of the above two papers. For example, reference [10] concludes that besides Te–Ge, Te–Sb and Ge–Ge pairs Sb–Sb bonds also exist in amorphous  $\text{Ge}_2\text{Sb}_2\text{Te}_5$ . The Sb–Sb coordination number is  $0.5 \pm 0.1$  and the mean Sb–Sb distance is 2.44 Å. Though this value is 0.46 Å shorter than the Sb–Sb bond length found in crystalline antimony, this result is not discussed any further in [10]. On the other hand Sb–Sb bonding is excluded in [11] and the uncertainty of coordination numbers is also significantly higher there (e.g.  $\langle N_{\text{Te}} \rangle = 2.4 \pm 0.6$ ).

From  $\langle N_{\text{Te}} \rangle$  it was concluded that ‘17% of Te atoms is over-coordinated’. We believe that the rather large freedom of interpretation and the uncertainty of coordination numbers ( $\pm 25\%$  for Te!) do not support such statements. It was also assumed that over-coordination of Te atoms results in the presence of ‘both twofold and planar threefold geometries’ [11]. This is inconsistent with the above value of  $\langle N_{\text{Te}} \rangle$ . If  $\langle N_{\text{Te}} \rangle$  is 2.4 and 17% of Te atoms is over-coordinated then the over-coordinated atoms should have 4 or 5 neighbours. Such high values have never been reported for glassy tellurides.

The present paper aims at the structural study of amorphous  $\text{Ge}_2\text{Sb}_2\text{Te}_5$ . One measurement (either diffraction or EXAFS) usually does not provide enough information for characterizing the short range order of a ternary amorphous alloy. An additional difficulty is that the difference of bond length values is rather small in amorphous  $\text{Ge}_2\text{Sb}_2\text{Te}_5$  (e.g.  $r_{\text{GeGe}} = 2.47$  Å,  $r_{\text{GeTe}} = 2.62$  Å [11]). Thus, to be able to determine the coordination numbers and interatomic distances (and to see clearly whether certain types of atoms are bonded at all) one needs the most comprehensive experimental information. In the case of  $\text{Ge}_2\text{Sb}_2\text{Te}_5$  it can be achieved by combining diffraction measurements (both neutron- and x-ray diffraction) with the three available EXAFS datasets.

EXAFS is element specific and gives accurate bond lengths but the uncertainty of the coordination numbers obtained by this technique is still relatively large. Diffraction data do not give strongly element specific information but due to the more precise normalization it may provide more accurate (neutron- or x-ray weighted) average coordination numbers. It can be expected that a model consistent simultaneously with both diffraction and EXAFS

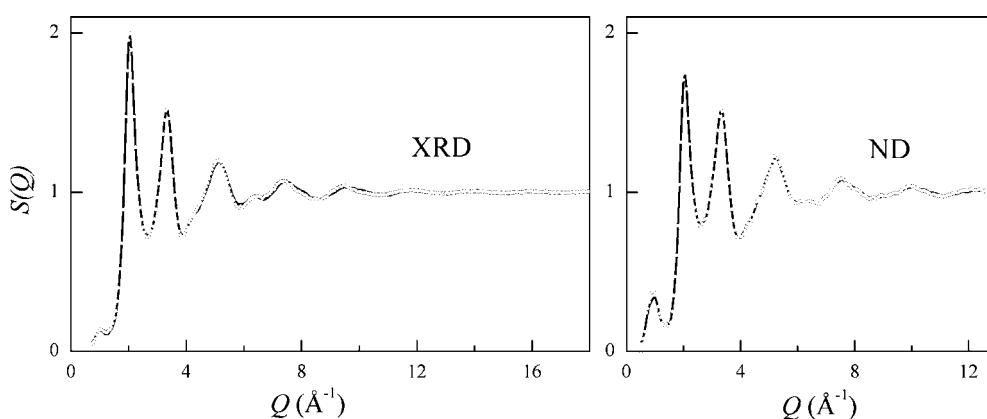


**Figure 1.** XRD and ND structure factors for sputtered amorphous  $\text{Ge}_2\text{Sb}_2\text{Te}_5$ . Circles—measured. Lines—obtained by simultaneous RMC simulation of the experimental XRD, ND and EXAFS data.

measurements will incorporate the advantages of these techniques. In other words it is possible to obtain element specific information due to EXAFS data while the uncertainty of coordination numbers and the possible correlations between variables deduced from an EXAFS fitting procedure is reduced by diffraction data. The number and accuracy of parameters that can be obtained from experimental data largely determines the reliability of modelling. The spatial resolution of diffraction data is discussed in detail in [12]. The extension to EXAFS and the estimation of the number of free fitting parameters is straightforward [13].

For this reason the five measurements are modelled simultaneously in the framework of the reverse Monte Carlo (RMC) simulation technique [14–16]. This method has two main advantages. First, several datasets can be fitted by one three-dimensional model ensuring the *internal consistency* of results. The second advantage is that chemical knowledge can also be incorporated in the models in the form of coordination constraints. RMC is used mostly to fit diffraction data but there are several studies on EXAFS measurements as well [17–19].

## 2. Experimental details

The investigated samples were prepared using DC magnetron sputtering. A thin film of thickness between one and three micrometres was sputtered on a Si-wafer coated with PMMA. The amorphous material was removed from the substrate by dissolving PMMA in acetone. Finally the flakes obtained were ground to a fine powder.

The x-ray diffraction experiment was carried out at the BW5 high energy beamline at HASYLAB, DESY, Hamburg. The energy of the incident beam was 100 keV ( $\lambda = 0.125 \text{ \AA}$ ). Scattered intensities were recorded by a Ge solid state detector. Raw data were corrected for background scattering, Compton scattering, polarization and variations of the detector solid angle [20].

The neutron diffraction measurement was carried out at the 7C2 liquid and amorphous diffractometer (LLB, Saclay). The wavelength of the incident beam was  $0.7 \text{ \AA}$ . About 600 mg of powdered  $\text{Ge}_2\text{Sb}_2\text{Te}_5$  sample was filled into a vanadium sample holder with 5 mm diameter and 0.1 mm wall thickness. Measured data were corrected for background, scattering from the sample holder, multiple scattering and absorption of the sample following standard procedures. X-ray and neutron diffraction structure factors are shown in figure 1.

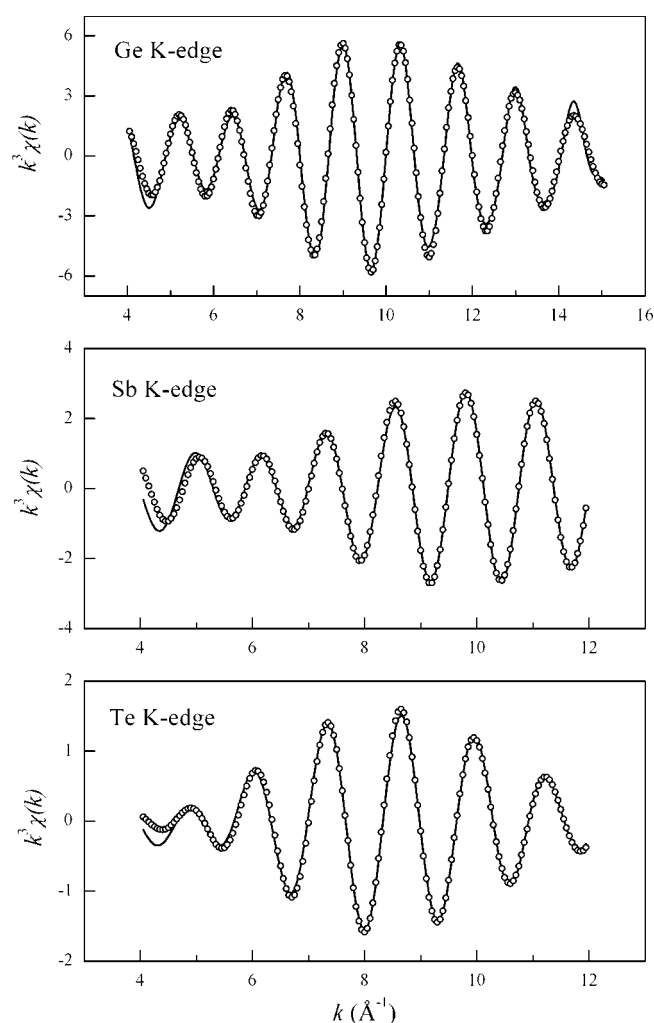


**Figure 2.** Ge-, Sb- and Te K-edge EXAFS curves for sputtered amorphous  $\text{Ge}_2\text{Sb}_2\text{Te}_5$ . Circles—measured. Lines—obtained by simultaneous RMC simulation of the experimental XRD, ND and EXAFS data.

EXAFS measurements were carried out at the X beamline of HASYLAB. Ground samples were mixed with polyethylene powder and pressed to tablets. Intensities were measured in transmission mode by ionization chambers filled with  $\text{N}_2$ –Ar mixture. The pressure and Ar content of the mixture was adjusted to the energy of the edge. Experimentally measured x-ray absorption cross sections were analysed using the program Viper [21]. Te-, Sb- and Ge K-edge EXAFS  $k^3\chi(k)$  curves are shown in figure 2.

### 3. Modelling

The reverse Monte Carlo simulation technique (RMC) is a robust and unsophisticated tool for generating large 3D models consistent with available structural information. For the simulation details, we refer to two recent papers [15, 16].

Simulations were carried out with a slightly modified version of the RMCA code [22]. The density was taken to be  $0.0315 \text{ \AA}^{-3}$  [23]. Initial configurations were obtained by hard sphere simulations satisfying cut off constraints only. Boxes for the test runs contained 4500 atoms. However, the final atomic configuration (or final set of pair distribution functions) was obtained with 36 000 atoms.

Several simulation runs were carried out starting from initial configurations satisfying different cut off distances. Ge–Te and Sb–Te bonds were allowed in each of these runs. To test the existence of ‘wrong bonds’ (not existing in the crystalline phase) in amorphous  $\text{Ge}_2\text{Sb}_2\text{Te}_5$  Ge–Ge, Sb–Ge, Sb–Sb and Te–Te bonds were allowed in all possible combinations.

Some runs were carried out to analyse the dependence of models on box size or initial configuration. Apart from statistical errors, the results did not depend on these factors at the level of coordination numbers and partial pair correlation functions.

EXAFS backscattering amplitudes and phases were calculated by the FEFF8 code [24] in the SCF (self-consistent field) approximation. To remain within the pair correlation function formalism of the RMC program all calculations were carried out with two atoms (absorber/backscatterer). This approximation is certainly inadequate for XANES calculations where multiple scattering involving two or more different backscatterers becomes predominant. However, in the present case, model calculations on small clusters (3–7 atoms) showed that backscattering amplitudes and phases are not sensitive to the presence of other atoms in the  $k$ -range used for fitting.

Throughout this paper the partial coordination numbers were calculated by integrating the radial distribution function  $4\pi r^2 \rho_0 c_j g_{ij}(r)$  up to the first minimum in the  $g_{ij}(r)$ .

#### 4. Results and discussion

It is known that crystalline forms of  $\text{Ge}_2\text{Sb}_2\text{Te}_5$  consist of two sublattices: Te atoms form one of them while Ge and Sb atoms with vacancies share the other one [25]. Thus, in spite of the large difference in their size and bonding nature, Ge and Sb play a similar role in the crystalline forms of  $\text{Ge}_2\text{Sb}_2\text{Te}_5$ . However, it is not necessarily true for the amorphous phase where symmetry does not force chemically different atoms to occupy similar positions. More generally, it can also be assumed that unlike other amorphous materials (e.g. a-Si or a-Se [26, 27]) the local order of crystalline and amorphous  $\text{Ge}_2\text{Sb}_2\text{Te}_5$  is different. In the metastable crystalline state Sb has 6 Te neighbours at about 3.006 Å. The mean Ge–Te distance (3.03 Å) is very close to that value but the first peak of  $g_{\text{GeTe}}(r)$  splits up [7]. The formation of homopolar bonds is avoided in the crystalline forms of  $\text{Ge}_2\text{Sb}_2\text{Te}_5$ .

If we assume that—similarly to the crystalline state—amorphous  $\text{Ge}_2\text{Sb}_2\text{Te}_5$  contains only Ge–Te and Sb–Te bonds *and* Sb and Ge has 3 and 4 Te neighbours then it follows that the average coordination number of Te is 2.8. Studies on glassy tellurides usually report much lower values [8, 9, 28, 29]. Thus at least one of the above conditions is not fulfilled in amorphous  $\text{Ge}_2\text{Sb}_2\text{Te}_5$ .

As the concentration of Te atoms in  $\text{Ge}_2\text{Sb}_2\text{Te}_5$  is as high as 56% the existence of Te–Te bonds was checked by the RMC modelling first. It was found that neither of the fits was improved by allowing Te–Te bonding. In the next step the formation of Ge–Ge bonds was tested in detail (with or without Te–Te, Sb–Sb and Sb–Ge bonds). The improvement of the fit of Ge K-edge EXAFS data was in all cases significant. The obtained Ge–Ge bond length (2.48 Å) is also very close to the value found in crystalline Ge. This agreement lends further support to the existence of Ge–Ge bonds. Ge–Ge bonding in amorphous  $\text{Ge}_2\text{Sb}_2\text{Te}_5$  was also reported in [10, 11].

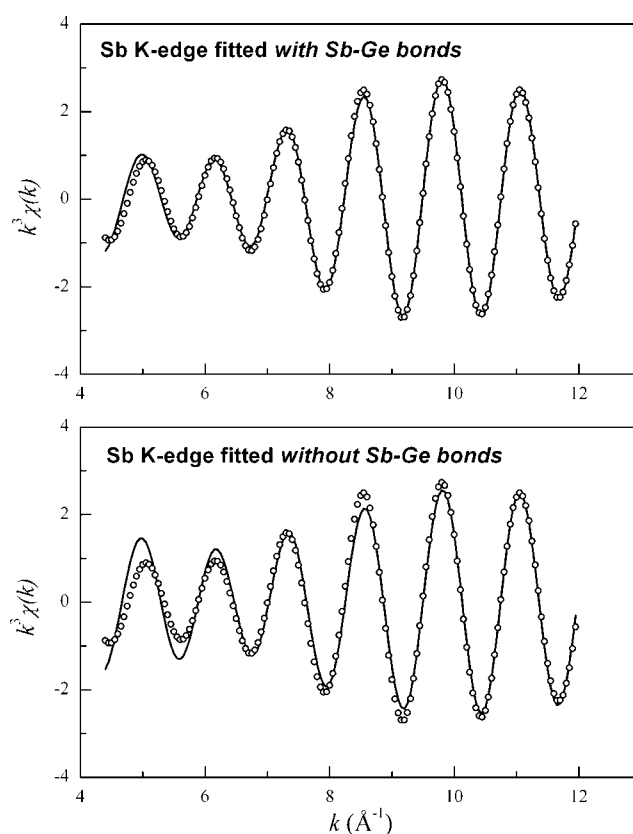


**Figure 3.** Sb K-edge EXAFS spectrum for sputtered amorphous  $\text{Ge}_2\text{Sb}_2\text{Te}_5$ . Circles—measured. Lines—obtained by simultaneous RMC simulation of the experimental XRD, ND and EXAFS data with and without Sb–Te bonds.

Introducing Sb–Sb bonding did not improve the quality of the fits. In some cases it was also observed that if Sb–Te, Te–Te and Sb–Sb bonding was allowed simultaneously then due to the similar scattering power of Sb and Te (both for x-rays and neutrons as well as for photoelectrons) the position of the corresponding peaks was inverted. For example the mean Te–Te distance was sometimes longer than the mean Sb–Te separation. As an overall experience of simulation runs it can be stated that neither Sb–Sb nor Te–Te bonding is needed for a good fit of available experimental data.

It was not possible to fit the Sb K-edge data without assuming Sb–Ge bonds. If all the other parameters remained the same then lowering the minimum Sb–Ge distance to 2.5 Å always resulted in a significant improvement of the fit quality (figure 3). The mean Sb–Ge distance is 2.69(0.02) Å, a value very close to the sum of covalent radii (2.68 Å). These findings together provide evidence that Sb–Ge bonding is present in the as-sputtered  $\text{Ge}_2\text{Sb}_2\text{Te}_5$ . Fits obtained by the simultaneous modelling of the 5 datasets assuming Te–Sb, Te–Ge, Ge–Ge and Sb–Ge bonding are shown in figures 1 and 2. The Sb–Ge coordination number is about  $0.83 \pm 0.1$  thus Sb–Ge bonding seems to play an important role in the structure of sputtered amorphous  $\text{Ge}_2\text{Sb}_2\text{Te}_5$ . However, we do not claim that Sb–Ge bonds can be found either in the liquid state or in melt quenched  $\text{Ge}_2\text{Sb}_2\text{Te}_5$ .

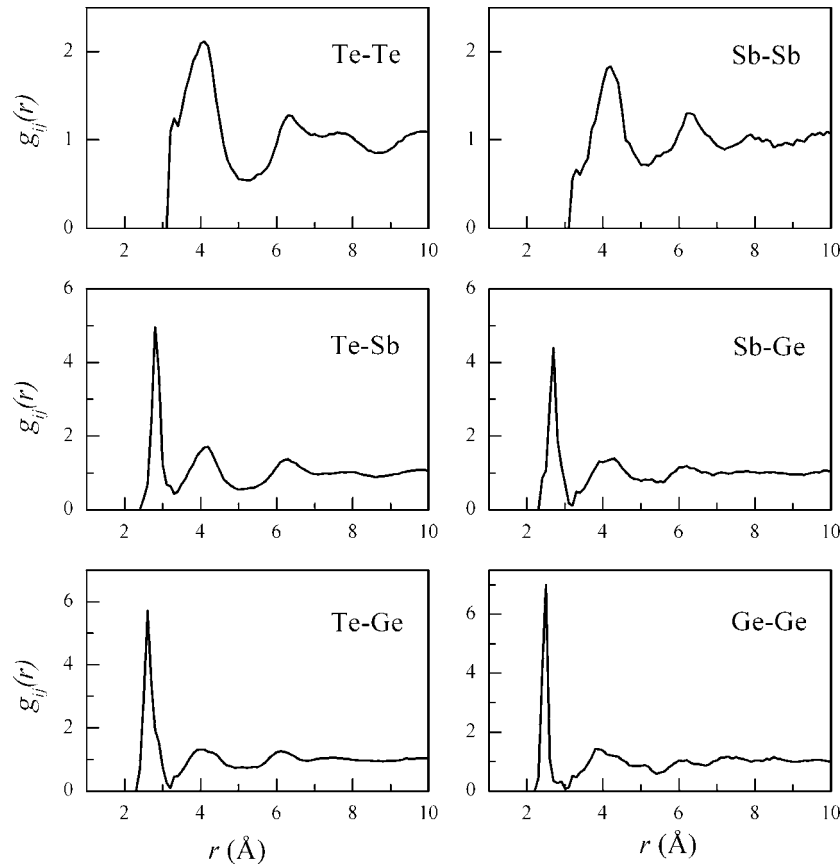


**Figure 4.** RMC simulated partial pair distribution functions for sputtered amorphous  $\text{Ge}_2\text{Sb}_2\text{Te}_5$ . See section 4 for details.

**Table 1.** Bond lengths and coordination numbers in as-sputtered amorphous  $\text{Ge}_2\text{Sb}_2\text{Te}_5$  obtained from an unconstrained simulation run. Coordination numbers are calculated up to the first minimum of the corresponding pair correlation function. Errors of bond lengths are given in brackets. The uncertainty of  $\langle N_{\text{Te}} \rangle$  is about 5% while that of  $\langle N_{\text{Sb}} \rangle$ ,  $\langle N_{\text{Ge}} \rangle$  and the partial coordination numbers is about 10%.

Pairs	Te-Sb	Te-Ge	Ge-Sb	Ge-Ge	$\langle N_{\text{Te}} \rangle$	$\langle N_{\text{Sb}} \rangle$	$\langle N_{\text{Ge}} \rangle$
Bond length (Å)	2.83(2)	2.64(2)	2.69(2)	2.48(2)	—	—	—
Coord. no.	0.96	1.08	0.83	0.69	2.04	3.22	4.24

The partial pair correlation functions obtained from an unconstrained simulation run (in which coordination numbers were allowed to change freely) are shown in figure 4 while bond lengths and coordination numbers are listed in table 1. The error of bond lengths is 0.02 Å. Due to the large Te content of the sample the uncertainty of  $\langle N_{\text{Te}} \rangle$  is about 5%. The uncertainty of  $\langle N_{\text{Sb}} \rangle$ ,  $\langle N_{\text{Ge}} \rangle$  and the partial coordination numbers is about 10%. According to our results the coordination number of Te is 2 within the experimental uncertainty, Sb has three nearest neighbours and Ge is fourfold coordinated. It was a rather general experience of the models that if good fits were obtained with reasonable bond length values then the coordination numbers were close to the ‘8-N’ rule [30]—even if they were not constrained.



Due to the presence of Ge–Ge and Ge–Sb bonds, the predominance of  $\text{GeTe}_{4/2}$  building blocks in the sputtered amorphous  $\text{Ge}_2\text{Sb}_2\text{Te}_5$  can safely be excluded. In [10, 11] a model was proposed in which sputtered amorphous  $\text{Ge}_2\text{Sb}_2\text{Te}_5$  is built up of  $\text{Te}_{3/2}\text{Ge}$ – $\text{GeTe}_{3/2}$  and  $\text{SbTe}_{3/2}$  motifs. On the basis of our results, the dominance of such motifs can also be excluded as the Ge–Ge coordination number is significantly smaller than one and there are a significant number of Sb–Ge bonds. Thus  $\text{Te}_{3/2}\text{Ge}$ – $\text{SbTe}_{2/2}$  and several other atomic arrangements can also occur. It is important to see that both diffraction and EXAFS data are sensitive to pair correlations and apart from some simpler cases they provide reliable information only at the level of two-body correlations. (This is not a deficiency of the simulation method applied—any other type of analysis/modelling relying on the above techniques would encounter this limitation.) Thus in ternary samples the existence of such motifs cannot be verified (only excluded) on the base of diffraction/EXAFS data.

## 5. Conclusions

The structure of sputtered amorphous  $\text{Ge}_2\text{Sb}_2\text{Te}_5$  was investigated by Te-, Sb- and Ge K-edge EXAFS, x-ray diffraction and for the first time neutron diffraction. The five datasets were modelled simultaneously by the reverse Monte Carlo simulation technique. The results obtained are thus consistent with all of the five measurements. Within the experimental errors the coordination number of Te, Sb and Ge is 2, 3 and 4, respectively. Thus, in contrast with the findings of some recent works on amorphous  $\text{Ge}_2\text{Sb}_2\text{Te}_5$  all atoms satisfy the 8-N rule. Besides Te–Ge and Te–Sb bonds present in the crystalline phases Ge–Ge and Sb–Ge bonding was also found to be significant.

## Acknowledgments

The x-ray diffraction and EXAFS measurements were supported by Deutsches Elektronen-Synchrotron, DESY. The neutron diffraction experiment was supported by the European Commission under the 6th Framework Programme through the Key Action: Strengthening the European Research Area, Research Infrastructures. Contract No. HII3-CT-2003-505925 supported by the European Access Programme to LLB-ORPHEE, Saclay. PJ was supported by the OTKA (Hungarian Basic Research Found) Grant No. T048580.

## References

- [1] Ovshinsky S R 1968 *Phys. Rev. Lett.* **21** 1450
- [2] Privitera S, Bongiorno C, Rimini E and Zonca R 2004 *Appl. Phys. Lett.* **84** 4448
- [3] Weidenhof V, Friedrich I, Ziegler S and Wuttig M 2001 *J. Appl. Phys.* **89** 3168
- [4] Kalb J A, Spaepen F and Wuttig M 2005 *J. Appl. Phys.* **98** 054910
- [5] Friedrich I, Weidenhof V, Njoroge W, Franz P and Wuttig M 2000 *J. Appl. Phys.* **87** 4130
- [6] Kolobov A V, Fons P, Frenkel A I, Ankudinov A L, Tominaga J and Uruga T 2004 *Nat. Mater.* **3** 703
- [7] Shamoto S, Yamada N, Matsunaga T, Proffen Th, Richardson J W Jr, Chung J-H and Egami T 2005 *Appl. Phys. Lett.* **86** 081904
- [8] Tani K, Yiwata N, Harigaya M, Emura S and Nakata Y 2001 *J. Synchrotron Radiat.* **8** 749
- [9] Hirota K, Nagino K and Ohbayashi G 1997 *J. Appl. Phys.* **82** 65
- [10] Baker D A, Paesler M A, Lucovsky G and Taylor P C 2006 *J. Non-Cryst. Solids* **352** 1621
- [11] Baker D A, Paesler M A, Lucovsky G, Agarwal S C and Taylor P C 2006 *Phys. Rev. Lett.* **96** 255501
- [12] Neufeind J 2001 *Phys. Chem. Chem. Phys.* **3** 3987
- [13] Kaban I, Gruner S, Jóvári P, Kehr M, Hoyer W, Delaplane R G and Popescu M 2007 *RMC 3 Proc.; J. Phys.: Condens. Matter* submitted
- [14] McGreevy R L and Pusztai L 1988 *Mol. Simul.* **1** 359

- [15] McGreevy R L 2001 *J. Phys.: Condens. Matter* **13** R877
- [16] Evrard G and Pusztai L 2005 *J. Phys.: Condens. Matter* **17** S1
- [17] Gurman S J 1995 *J. Synchrotron Radiat.* **2** 56
- [18] Gurman S J and McGreevy R L 1991 *J. Phys.: Condens. Matter* **2** 9463
- [19] Winterer M 2004 *J. Appl. Phys.* **88** 5635
- [20] Poulsen H, Neuefeind J, Neumann H B, Schneider J R and Zeidler M D 1995 *J. Non-Cryst. Solids* **188** 63
- [21] Klementev K V 2001 *J. Phys. D: Appl. Phys.* **34** 209
- [22] McGreevy R L, Howe M A and Wicks J D 1993 RMCA version 3; available at <http://www.isis.rl.ac.uk/RMC/rmca.htm>
- [23] Njoroge W K, Wöltgens H and Wuttig M 2002 *J. Vac. Sci. Technol. A* **20** 230
- [24] Ankudinov A L and Rehr J J 2000 *Phys. Rev. B* **62** 2437
- [25] Nonaka T, Ohbayashi G, Toriumi Y, Mori Y and Hashimoto H 2000 *Thin Solid Films* **370** 258
- [26] Gereben O and Pusztai L 1994 *Phys. Rev. B* **50** 14136
- [27] Jóvári P, Delaplane R G and Pusztai L 2003 *Phys. Rev. B* **67** 172201
- [28] Jóvári P, Kaban I, Hoyer W, Delaplane R G and Wannberg A 2005 *J. Phys.: Condens. Matter* **17** 1529
- [29] Abe K, Uemura O, Usuki T, Kameda Y and Sakurai M 1998 *J. Non-Cryst. Solids* **232–234** 682
- [30] Mott N 1967 *Adv. Phys.* **16** 49